In-situ plasma treatment of Cu surfaces for reducing the generation of vacuum arc breakdowns

Saressalo, Anton

American Institute of Physics
2021-10-14

Saressalo, A, Kilpeläinen, A, Mizohata, K, Profatilova, I, Nolvi, A, Kassamakov, I, Tikkanen, P O, Calatroni, S, Wuensch, W & Djurabekova, F 2021, 'In-situ plasma treatment of Cu surfaces for reducing the generation of vacuum arc breakdowns', Journal of Applied Physics, vol. 130, no. 14, 143302. https://doi.org/10.1063/5.0062674

http://hdl.handle.net/10138/335285
10.1063/5.0062674

unspecified
acceptedVersion

Journal of Applied Physics

In-situ plasma treatment of Cu surfaces for reducing the generation of vacuum arc breakdowns

Cite as: J. Appl. Phys. **130**, 143302 (2021); https://doi.org/10.1063/5.0062674
Submitted: 07 July 2021 . Accepted: 26 September 2021 . Published Online: 12 October 2021

Anton Saressalo, Aarre Kilpeläinen, Kenichiro Mizohata, et al.

Journal of Applied Physics ARTICLE scitation.org/journal/jap

In-situ plasma treatment of Cu surfaces for reducing the generation of vacuum arc breakdowns

Cite as: J. Appl. Phys. **130**, 143302 (2021); doi: 10.1063/5.0062674
Submitted: 7 July 2021 · Accepted: 26 September 2021 ·
Published Online: 12 October 2021

Anton Saressalo,[1,a)] Aarre Kilpeläinen,[2] Kenichiro Mizohata,[2] Iaroslava Profatilova,[3] Anton Nolvi,[2] Ivan Kassamakov,[2] Pertti Tikkanen,[2] Sergio Calatroni,[3] Walter Wuensch,[3] and Flyura Djurabekova[1]

AFFILIATIONS

[1]Helsinki Institute of Physics and Department of Physics, University of Helsinki, PO Box 43 (Pietari Kalmin katu 2), 00014 Helsingin yliopisto, Finland
[2]Department of Physics, University of Helsinki, PO Box 43 (Pietari Kalmin katu 2), 00014 Helsingin yliopisto, Finland
[3]CERN, European Organization for Nuclear Research, 1211 Geneva, Switzerland

[a)]**Author to whom correspondence should be addressed:** anton.saressalo@helsinki.fi

ABSTRACT

High electric fields are present in a rapidly growing number of applications, which include elementary particle accelerators, vacuum interrupters, miniature x-ray sources, and satellites. Many of these applications are limited by the breakdown strength of the materials exposed to electric fields. Different methods have been developed to improve the quality of metal electrode surfaces, aiming to increase their breakdown strength. Not many systematical studies have been performed to provide a proper understanding of what contributes to the correlation between the breakdown strength and the quality of the surface. In this work, we apply a novel method for reducing vacuum arc breakdowns by cleaning the electrode surfaces with O and Ar plasma. The method can be used to alter the surfaces of the Cu electrodes *in situ*, i.e., without exposing them to air between the measurements. This plasma cleaning treatment is shown to reduce the number of surface impurities and to speed up the conditioning process of the samples under high-voltage pulses. Specifically, the first breakdown field was observed to increase by more than 90% after the plasma cleaning.

I. INTRODUCTION

Physical properties of metal surfaces may depend on their level of chemical purity. Pure metal surfaces are typically extremely reactive: a layer of impurities is formed within nanoseconds when such a surface is exposed to air. Even in ultrahigh vacuum ($P = 1 \times 10^{-7}$ Pa), a monolayer of gas residuals may deposit on the clean surface in a matter of minutes.[1]

Various cleaning techniques have been developed over the centuries in order to distinguish the effects of the surface impurities from those caused by the underlying material. Examples of such laboratory cleaning methods include chemical degreasing with solvents. These may be combined with mechanical vibrations such as ultrasonic waves or with blazing the unwanted material away with lasers.[2–5] Some of these methods are easily accessible in most research laboratories, while some require advanced equipment to perform.

A common drawback of many of these methods is that they have to be performed in a separate apparatus and, therefore, it is often impossible to transport the samples into another research system without exposing them to the atmosphere, thus at least partially contaminating the surfaces in between. Avoiding the atmospheric exposure requires a specific design of the equipment in such a way that the sample preparation can be done directly in the same environment as the actual experiments.

Earlier research shows that one surface-sensitive phenomenon is the ignition of vacuum arcs between copper electrodes in vacuum.[6,7] Also known as breakdowns (BDs), these short-circuit events are a major limiting factor in various apparatuses involving high electric fields.

The variety of applications using high electric fields ranges from elementary particle accelerators and tabletop x-ray sources to

vacuum interrupters, satellites, and medical appliances.[8–12] High electric fields are required in various charged particle accelerators to minimize the apparatus size—and thus the construction and operating costs.

The processes leading to the onset of vacuum plasma have been studied for more than a hundred years,[1,13–15] but still there is no consensus on the relative importance of surface impurities compared to processes triggered within the material on the breakdown generation. There are several indications that the breakdowns are linked to intrinsic effects, such as dislocations in the subsurface region.[16–18] Recent studies have shown how these mechanisms can lead to the formation of runaway processes, eventually creating a conducting plasma channel between the electrodes.[19–21] Plasma cleaning has been shown to improve the performance of a tandem particle accelerator functioning in the megavolt range.[22]

In this work, we apply oxygen and argon plasma treatment on copper electrodes and study the resulting changes in the surface morphology and elemental composition. Furthermore, the plasma treatment is combined with vacuum arc breakdown experiments in order to bring light to the extent of the effects of the surface impurities on the BD generation and to review potential methods for improving the breakdown resistance of copper structures. The effects are investigated by studying the surfaces modifications and by comparing the conditioning curves of Cu electrode pairs with and without the plasma treatment.

II. EXPERIMENTAL METHODS

A. Electrodes

Hard and soft Cu electrodes are used in the experiments since they are known to be conditioned differently.[23] Both sample types are oxygen-free high-purity electronic copper, diamond-machined in the shape of cylindrical electrodes. Hard Cu has a grain diameter between 10 and 100 μm (at least 4 by the ASTM E112 Standard[24]). Soft Cu samples experience an additional heat treatment, first at 1040 °C in the hydrogen atmosphere, and subsequently at 650 °C in vacuum to breathe out hydrogen. Based on the Heyn Linear Intercept procedure described in the ASTM E112 Standard, the average grain diameter of the used soft Cu was estimated to be $2.1 + 0.6$ mm.

In these experiments, we used several pairs of circular electrodes with the diameter of the contact area either 40 or 60 mm depending on the setup. Similar electrodes are described in more detail in Refs. 25 and 23. In most measurements, the anode had a smaller diameter than the cathode to minimize the field enhancement near the edges of the electrodes, which is seen in the BDs clustering within a few millimeters from the edge.[25] In the experiments performed in Helsinki, the gap length between the electrodes was 40 μm, while for the one pair, measured at CERN, both the anode and the cathode had the same diameter of 40 mm and the gap was 60 μm. A modified geometry was required to allow BD localization at the measurements performed at CERN.[26] Previous experience has shown that changing the gap size did not significantly affect the BD generation, except for the obvious difference in the electric field strength.[27] This is why we decided to include in this analysis not only the electrodes used in the single system, but also those which were tested at CERN. Since in this study, we focus on the quality of the cathode surface as a prime source of field emission currents resulting in BD events, the electrode polarity remained unchanged throughout the study, i.e., the bottom electrode was used as a cathode during both the plasma treatment and the BD experiments.

TABLE I. The electrode pairs used in the measurements. The third column shows the diameters of anode/cathode in mm.

ID	Material	Geometry	Gap (μm)	Experiments
A	Hard Cu	60/60	40	Plasma cleaning, SWLI
B	Hard Cu	40/60	40	Plasma cleaning, ERDA, conditioning, reconditioning
C	Hard Cu	40/60	40	Conditioning (reference)
D	Soft Cu	40/60	40	Plasma cleaning, microscopy, conditioning
E	Soft Cu	40/40	60	Conditioning (reference)

The electrode types and geometries used in each measurement are listed in Table I.

B. Plasma treatment

The plasma treatment is performed by inserting the electrodes into a Large Electrode System (LES) vacuum chamber,[25] which was modified to allow gas flow while under vacuum. A schematic of the system is presented in Fig. 1. During the plasma experiments, the Marx generator, which is used for electric pulsing (see Sec. II D) and the constant dc voltage, is controlled directly by the power supply.

The plasma is created by feeding the chamber with a selected gas and applying a dc voltage across the gap to ionize the gas molecules. Both oxygen (>99.9999% purity) and argon (>99.99% purity) gases were used to clean the electrode surfaces. The oxygen plasma is aimed to clean the surface from various hydrocarbons, while argon plasma is used for removing the excess oxygen from the surface.[28]

The treatment was executed by the following procedure:

1. Pump the LES chamber into high vacuum (<1 mPa). To remove traces of air molecules from the system.
2. Flush the chamber with oxygen or argon gas until the target pressure is reached (1 kPa for O and 6 kPa for Ar).
3. Apply a dc voltage across the gap and increase its value until the plasma onset, i.e., when a stable current in the mA range is observed, indicating the formation of a conducting plasma channel between the electrodes. The resulting glow can also be confirmed visually through the chamber windows.
4. Maintain a constant target voltage and current to preserve the plasma for 10 min.
5. Switch off the voltage and pump the chamber back to high vacuum. Repeat steps 2–5 when another gas is used.

In the experiments, the plasma current was capped to the glow discharge region (200 mA, 160A/m^2); thus, this was the value of the current most of the time the plasma was on. The value of the applied voltage was determined by the Paschen's curve, as discussed in Sec. III A.

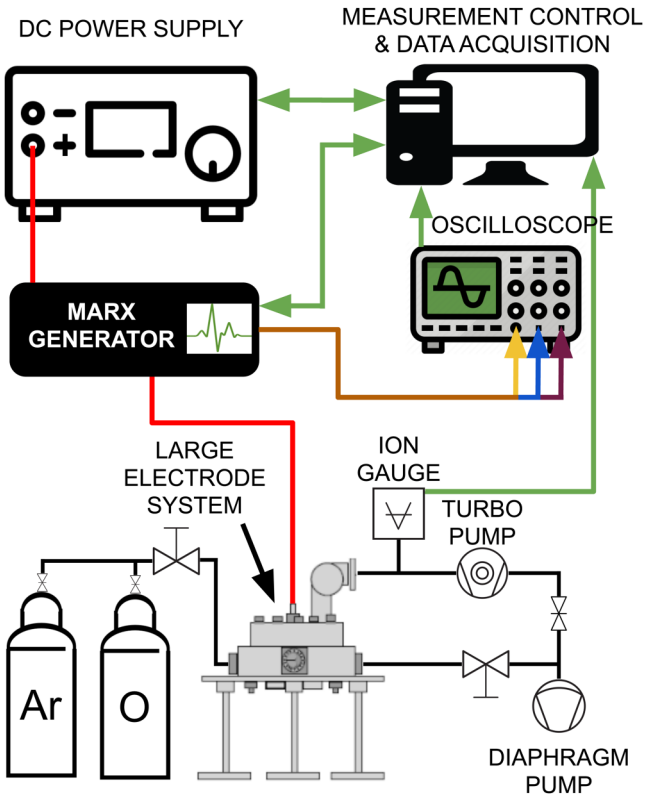

FIG. 1. A schematic of the pulsed dc system, modified to enable gas flow used in the measurements. Red lines depict the HV cabling, black lines depict the gas and vacuum piping while the other colors portray electric data signals between the devices.

In some experiments, either only oxygen or only argon plasma was used to understand the effects of either of the treatments separately. The optimal pressures for both gases were found experimentally for maximizing the stability of the plasma.

C. Surface analysis

To understand the effects of the plasma treatment, the elemental composition of the electrode surfaces was studied. The surfaces were also imaged optically in both macro and micro-scale and the topography of the surfaces was analyzed.

The elemental analysis of the surfaces was performed after each plasma cleaning stage by Elastic Recoil Detection Analysis (ERDA) with 40 MeV $^{117}I^{7+}$ ions, using a 5 MV tandem accelerator at the University of Helsinki.[29] The technique averages the elemental composition over a roughly $1 \times 1\,mm^2$ area on the surface.

The ERDA was performed for the hard Cu (pair B) samples at five stages:

#1 Pristine electrodes
#2 After oxygen and argon plasma treatment and a subsequent weekend in vacuum
#3 Immediately after oxygen and argon plasma treatment
#4 Immediately after oxygen plasma treatment
#5 Immediately after argon plasma treatment

Pristine refers to unused electrodes in the state they were taken from the storage in N_2 atmosphere. The samples had to be removed from the LES chamber and exposed to air for at least half an hour between the plasma treatment and the ERDA.

In addition, the samples were optically imaged. Pictures were taken both from the entire electrode surfaces and from the specific microscopic spots after each stage. The soft Cu electrodes (pair D) were imaged in the following order:

(a) Pristine electrodes
(b) After argon plasma treatment
(c) After oxygen plasma treatment
(d) After oxygen and argon plasma treatment and subsequent conditioning

The plasma-cleaned electrode surfaces of pair A were also imaged with a Scanning White Light Interferometer (SWLI), which can image nanometer-scale height changes in the surface topology, covering a large surface area in a single image.[30]

D. Breakdown measurements with a pulsed DC system

In this study, the main application of the plasma treatment was to study the effect on the BD resistance of the electrodes. The LES setup allowed to perform the plasma cleaning and a subsequent switch to BD generation with dc pulses without exposing the electrodes to vacuum in between.

The BD experiments were carried out with nearly identical Pulsed DC Systems at the University of Helsinki and at CERN. In addition to the LES vacuum chamber, the system includes a power supply, a Marx generator,[31] an oscilloscope, and an ion gauge for vacuum pressure measurement.[25,26] A schematic of the full system can be seen in Fig. 1.

In the experiments, two pairs of pristine hard Cu and two pairs of pristine soft Cu electrodes (pairs B–E, respectively) were conditioned using electric pulses and BDs. Prior to exposure to any HV pulses, one pair of each type underwent the plasma treatment process (first with O, then with Ar), and a reference pair was conditioned without the treatment.

Additionally, the plasma cleaned hard Cu pair was exposed to additional reconditioning experiments both with and without a preceding plasma cleaning. This was done to understand the long-term effects of the plasma cleaning after extended idle time in vacuum and in air.

In the measurements, the Marx generator was used for producing square dc pulses with voltages up to 6 kV (150 MV/m with a 40 μm gap), with a frequency of 2 kHz and with a pulse width of 1 μs. Also, the detection of the BD events was performed by the Marx generator: when the maximum value of the measured current during a voltage pulse was greater than the displacement current required to charge the electrodes, a BD event was registered and the pulsing was immediately stopped. More details of the system and BD detection are discussed in Ref. 25.

Differing from the other measurement geometries, a 60 μm gap and 40 mm cathode against 40 mm anode was used with the soft Cu pair E that was conditioned without plasma cleaning. The electric field strength E across the different gap sizes d was estimated simply from the voltage V by assuming $E = V/d$, as argued by Ref. 23. It has been shown that an exact comparison between different gap sizes should take into account other effects than only the increasing electric field strength.[27] This matter is discussed in the Appendix.

The pulsing voltage was determined by the feedback algorithm, in which the voltage is increased after every pulsing period of 1 00 000 pulses with no BD. If a BD occurred during the pulsing period, the voltage was either kept constant or decreased based on the number of pulses in the period. The algorithm is described in more detail in Refs. 25 and 26.

III. RESULTS

A. Plasma characteristics

Since the gas discharge glows evenly only within a specific range of gas pressure and voltage, we studied the onset voltage between the two electrodes (pair B in Table I) as a function of gas pressure for both oxygen and argon gases. The results are shown in Fig. 2. However, while the Paschen characteristics were used as a baseline for the most optimal pressure, the pressures used during the plasma treatments were chosen by finding the pressure with the most stable current plasma glow.

For oxygen, the trend follows the Paschen curve[32] and there is a clear minimum in the onset voltage near the pressure of 10 kPa or pd of 0.5 Pa m, which is similar to the values seen in other experiments with dc oxygen plasma, also in a micro-gap.[33] At higher pressures, the onset voltage increases rapidly.

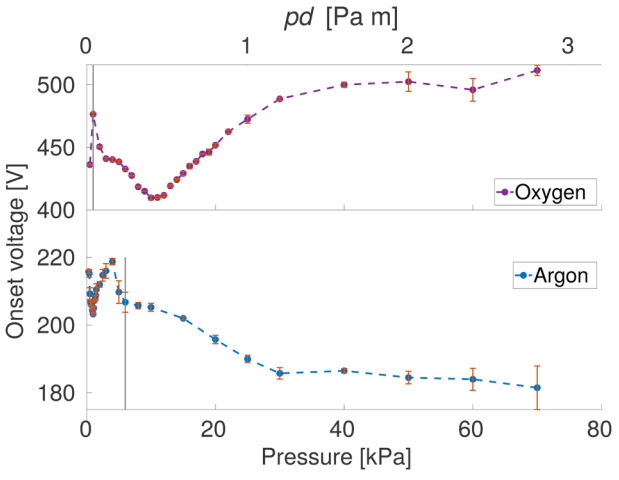

FIG. 2. Onset voltages for oxygen and argon plasma forming between the electrodes (pair B) as a function of pressure. Each point is a mean value over four measurements. The uncertainties are estimated from the standard error of the mean. The top x-axis scale presents the pressure (p) multiplied by the distance (d) of 40 μm across the gap, while the bottom x-axis indicates the corresponding pressure. The vertical lines indicate the chosen pressures for the plasma treatment with each gas.

For argon, no clear minimum was found. Instead, the onset voltage steadily decreases as the pressure increases, which is in line with theoretical predictions.[34] We observe a significant slowdown in the decrease rate above 30 kPa but, unfortunately, the upper pressure limit of the experimental setup (70 kPa) did not allow us to identify the global minimum near this pressure, as suggested in Ref. 35.

B. Plasma cleaning effect on electrode surfaces

To verify the cleaning effect of the plasma treatment, the Cu surfaces of electrode pair B (Table I) were analyzed by measuring the concentrations of impurity elements. The surfaces were also analyzed visually and the height profile was measured with an SWLI profilometer.

The ERDA results of the surface concentrations on the pristine hard Cu electrodes are presented in Table II. Relative changes to these initial concentrations are visualized in Fig. 3. The surfaces were analyzed in the order described in Sec. II C. The detected impurity elements were hydrogen, carbon, nitrogen, oxygen, and sulfur.

In Table II and Fig. 3, we observe that initially (see the blue bars marked in the legend of Fig. 3 as "ERDA #1") the surface concentrations are very similar on the cathode and the anode. After the first plasma cleaning with oxygen and argon, the second ERDA measurements (the orange bars "ERDA #2" in Fig. 3) did not reveal significant changes in the impurity concentrations on the surfaces of either the cathode or the anode. Since the ERDA measurement was carried out with a delay of 3 days after the plasma cleaning, we concluded that the surface cleaning may have been degraded due to possible residual molecules in the vacuum. Hence, in the next experiment shown in the yellow bars ("ERDA #3") in Fig. 3, the electrodes were analyzed immediately after the plasma treatment. Here, we see a decrease in the concentrations for all the elements.

The next surface analysis was performed immediately after a plasma cleaning with only oxygen (the violet bars "ERDA #4" in Fig. 3). We see that this was detrimental for the surface, as it did not only substantially increase the amount of oxygen, but also the amount of all other elements except nitrogen. Presumably, the reactive residual oxygen molecules actively attracted impurities from the air between the plasma treatment and the ERDA measurement.

TABLE II. Surface concentrations of the detected elements on the pristine hard Cu electrodes (pair B) measured with ERDA.

	Surface concentration (10^{15} atoms cm^{-2})				
	H	C	N[a]	O	S
Cathode	1.9 ± 0.4	1.8 ± 0.3	0.5 ± 0.1	7.9 ± 0.5	1.2 ± 0.2
Anode	1.4 ± 0.4	1.4 ± 0.2	0.3 ± 0.1	6.9 ± 0.4	0.8 ± 0.1

[a]The values for N are from the measurement#3, i.e., after the first O+Ar plasma cleaning since no nitrogen was detected on the pristine electrodes. The uncertainties are given as standard deviations.

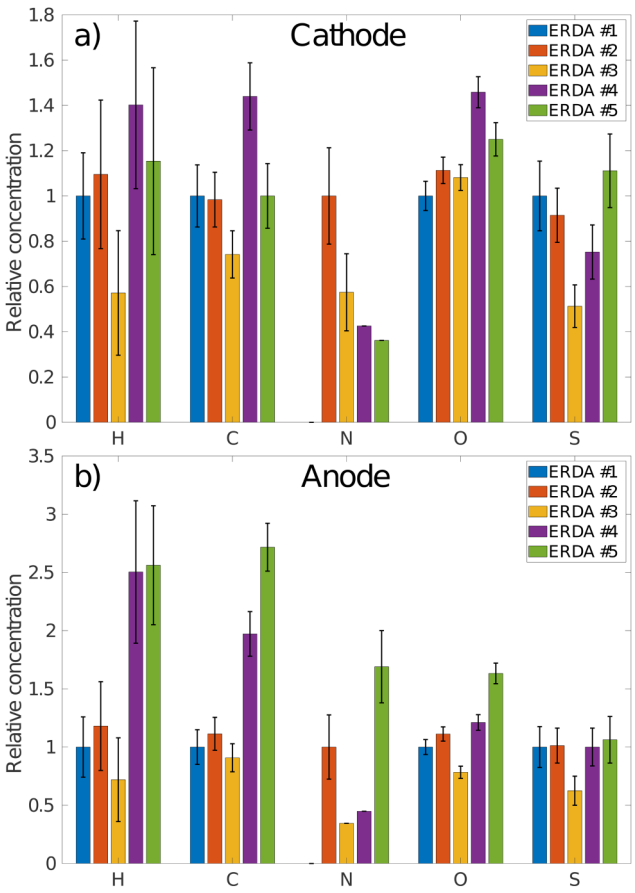

FIG. 3. Relative changes in the hard Cu (pair B) surface concentrations detected by ERDA on (a) cathode and (b) anode of the hard Cu electrode pair. The ERDA measurements were performed in the following order: #1: Pristine electrodes, #2: After O+Ar plasma and a weekend in vacuum, #3: Immediately after O+Ar plasma, #4: Immediately after O plasma #5: Immediately after Ar plasma. The values are grouped by elements and are relative to the concentrations measured on the pristine electrodes (blue bars), which are presented in Table II. The uncertainties are given as standard deviations.

The last measurement (the green bars "ERDA #5" in Fig. 3) was done immediately after the treatment only with argon plasma. The results show that the treatment decreased the concentrations of all the elements except S as compared to the oxygen-treated surface. Whereas the composition of the contamination on the anode surface remained mainly intact or even worsened compared to the values after the oxygen treatment. This suggests that the plasma cleaning strongly affected the cathode surface. Since the effect of argon plasma cleaning on the anode surface was negligible, this surface (still oxygen-rich after the oxygen plasma cleaning) was naturally exposed to air for approximately twice as long as the cathode surface. The time between the O plasma and ERDA #4 and between Ar plasma and ERDA #5 were approximately the same. This could explain the lower purity of the anode surface in the last measurement. Additionally, the atoms sputtered from the cathode due to the plasma, may land on the anode, introducing additional impurities and irregularities.

The plasma-treated soft Cu electrodes (pair D in Table I) were imaged after each cleaning stage, as listed in Sec. II C. Images of the cathode after each of those stages are shown in Fig. 4. Optical microscopy images from a spot near the center of the cathode are shown in Fig. 5.

A clear difference between the quality of the cathode surface before and after plasma cleaning is seen in the comparison of Figs. 4(a) and 4(b). Here, the 40 mm diameter circle centered on the cathode surface, which was separated from the anode by 40 μm gap, was exposed to the Ar plasma cleaning. From this comparison, we conclude that the Ar plasma is able to improve the reflectivity of the Cu surface. In Fig. 4(c), the hue of this circular area changes again toward the red shade after the O plasma cleaning, which indicates an increase in oxidation on the surface. Also in this image, some highly reflective spots appear on the surface. In Fig. 4(d), we see the white-colored BD spots, which appear uniformly, without clustering, across the whole 40 mm contact area.

High-resolution optical image of the cathode (pair D in Table I) surface shown in Fig. 5 does not reveal any visible changes after the Ar plasma cleaning [compare Figs. 5(a) and 5(b) that show the cathode surface before and after Ar plasma cleaning, respectively]. However, after O plasma cleaning, several white spot areas [one shown in Fig. 5(c)] appear on the surface. These are the same reflective spots that are seen in the full surface image in Fig. 4(c). In Fig. 5(d), we show the same spot after the conditioning

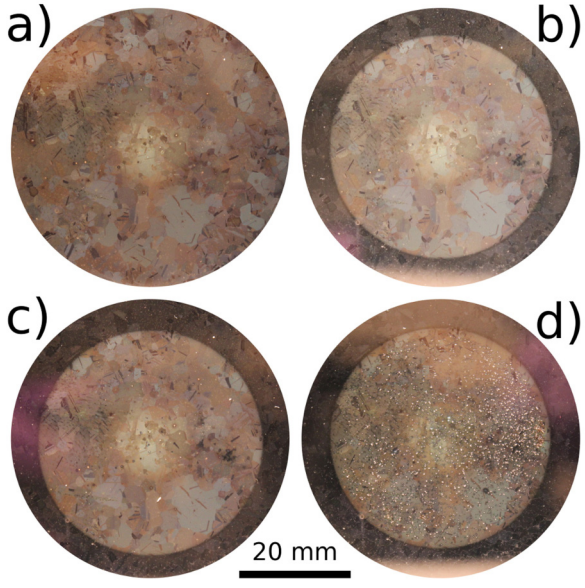

FIG. 4. 50 mm diameter area in the center of the cathode surface of the soft Cu electrode (pair D) (a) before plasma treatment, (b) after Ar plasma treatment, (c) after O plasma treatment, and (d) after O+Ar plasma treatment and subsequent conditioning.

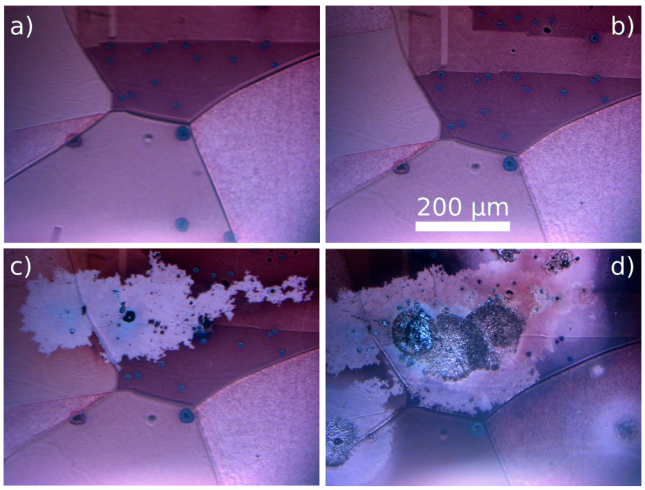

FIG. 5. The same spot on the soft Cu (pair D) cathode imaged (a) before plasma treatment, (b) after Ar plasma treatment, (c) after O plasma treatment, and (d) after O+Ar plasma treatment and subsequent conditioning.

experiment. Although the Ar plasma has preceded the conditioning experiment, the white spot did not shrink. On the contrary, it grew in size, filling up the entire surface of the grain, which it was covering initially only partially. A few breakdown spots are visible in the middle of this expanded white spot area. We note the irregular shape of these white spot area, resembling the random walk pattern observed for arc plasma,[36] and hence suggesting the origin of the white spot to be from the plasma surface interaction.

Additionally, the height profile of a hard Cu (pair A in Table I) cathode surface was scanned with the optical and SWLI microscopes. The measurement was made after the various plasma treatments with argon and, most recently, with oxygen. The resulting height profile of one area of the surface is shown in Fig. 6. The profile shows a typical cathode BD crater with a somewhat elevated ring area in its immediate vicinity and a more irregular surface further away from the crater. Two patches of elevated islands are visible in the top-right corner of Figs. 6(a) and 6(b), which are similar in reflectivity to those seen on the soft Cu surface after the oxygen plasma treatment, presented in Fig. 5(c). More close inspection of Fig. 6(c) shows that the elevated ring area around the crater keeps the shape of the groves remaining from the diamond machine treatment of the surface. Moreover, the height of the ridges between the groves is very similar to the height of the tall ridges on the pristine surface. This indicates that the surface around the crater was also strongly heated, but only slightly affected by the plasma itself. The plasma bombardment could have caused the grooves on the surface to become shallower, as seen in the figure.

C. Effects on BD generation

As the main purpose of the plasma cleaning was to study its effect on the BD probability, we performed conditioning of the plasma-treated hard and soft Cu electrodes (pairs B and D in

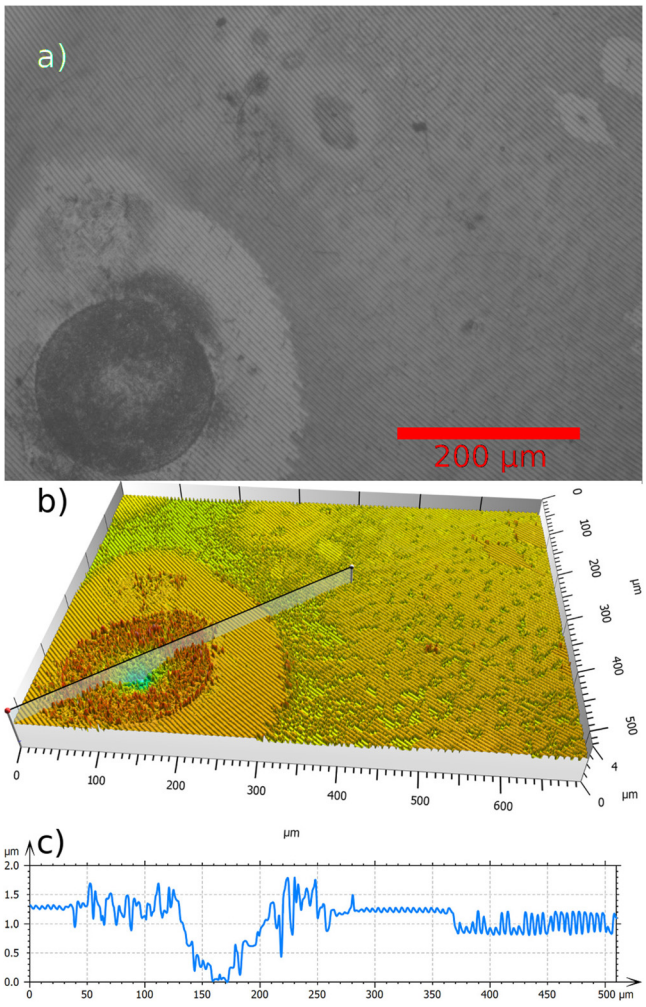

FIG. 6. (a) An optical microscope image of an area on a hard Cu cathode (pair A) surface after plasma treatment with oxygen. (b) Topography map of the same area. The color coding shows the surface height profile obtained by an SWLI microscope, with the red features being the highest and the blue ones the lowest. (c) Height profile along the line shown in (b). The profile depicts a BD crater and the area around it.

Table I) with high-voltage dc pulses while controlling the breakdown rates. The resulting conditioning curves from these experiments are compared to the untreated hard and soft Cu samples (pairs C and E in Table I). If the electrodes were not yet exposed to high-voltage pulses and did not experience BDs, we specify the conditioning of such surfaces as *initial* to distinguish it from the reconditioning process, i.e., the conditioning of the previously conditioned electrodes that were exposed to air after the initial conditioning. The initial conditioning results are presented in Fig. 7(a). Since one of the conditioning experiments was performed with the gap of a different size, it is important to take into account the scaling of the electric field in the gap with the gap size d as $\frac{1}{d^{0.7}}$

rather than as $\frac{1}{d}$ ($E = V/d$, where E stands for the electric field and V for the electric bias between the electrodes) as it was shown in Refs. 27 and 37. We have analyzed the possible difference, but found that within the small gap sizes used in our experiments, the accurate scaling does not significantly affect the shape of the curves in Fig. 7(a) (see Fig. 9 in the Appendix). Thus, the simpler scaling is used here so that the units are comparable with the other measurements.

We see that after the plasma treatment, there are fewer BDs during the initial pulses, compared to the measurements without the treatment. For hard Cu, the conditioning curves overlap at above 1×10^8 pulses, which corresponds to approximately 1000 BDs. Because of the feedback algorithm (Sec. II D), this leads to a steeper rise in the electric field during the first 10^8 pulses. For the soft Cu experiments, the overlap occurs much later, at around 5×10^8 pulses (5000 BDs). Crucially, the first BD occurred at almost double the electric field strength (60 MV/m for hard Cu and 23 MV/m for soft Cu after the treatment compared to 31 MV/m for hard Cu and 12 MV/m for soft Cu without the treatment). In general, the average values for the first BD fields measured in the LES setups in Helsinki and CERN for numerous Cu surfaces (without plasma treatment) are (35 ± 5) MV/m for hard Cu (six pairs) and (15 ± 3) MV/m for soft Cu (seven pairs), uncertainties are given as standard deviations.

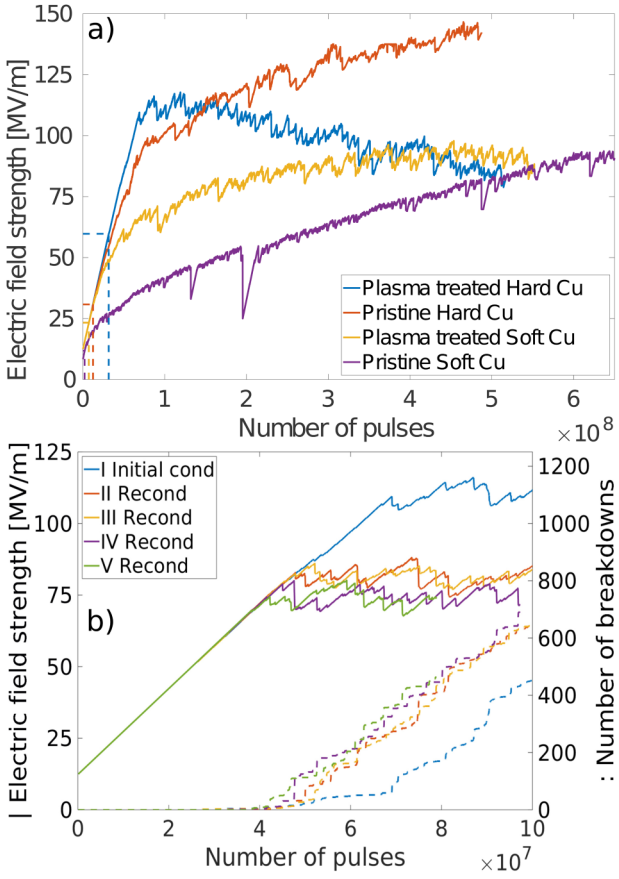

FIG. 7. (a) Electric field strength against the number of pulses (solid lines) of the initial conditioning experiments for electrode pairs with and without plasma cleaning (pairs B–E, respectively). The dashed lines show the pulse number and the electric field strength of the first BD in each measurement. (b) Comparison of the initial conditioning of the plasma-treated hard Cu sample (pair B) against subsequent reconditioning measurements described in Table III. The dashed lines indicate the number of BDs as a function of the number of pulses.

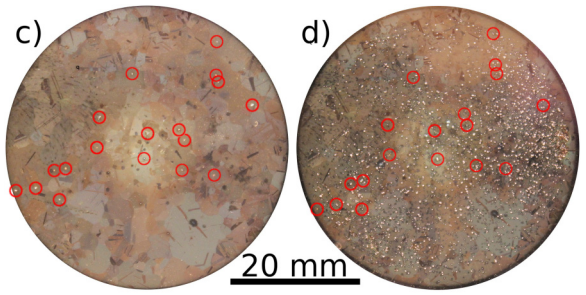

FIG. 8. Soft Cu (pair D) cathode (c) after O plasma cleaning, (d) after subsequent conditioning and BDs as seen in Fig. 4, but with the 18 most prominent reflective spots highlighted.

In Fig. 7(a), we observe that after the initial steep growth of the voltage, the curve of the plasma-cleaned hard Cu starts decreasing. The decrease goes from the peak field of 120 MV/m down to 80 MV/m, which is also the field achieved by the later reconditioning runs, as seen in Fig. 7(b). This type of de-conditioning is not typically seen during the initial conditioning process and could result from surface activation due to the plasma treatment.[38] Also, the vacuum level in the gap was almost by an order of magnitude poorer due to the modifications in the system, which were necessary to allow the gas flow for the plasma cleaning: 5×10^{-5} Pa compared to the usual $\sim 7 \times 10^{-6}$ Pa. This decreasing trend is not seen in the initial conditioning curve of the plasma cleaned soft Cu. As the soft Cu conditioning happens slower,[23] this de-conditioning effect might be just seen as even slower conditioning. Regardless, the final electric field strength after 5×10^8 pulses is very similar for both the plasma-treated samples.

TABLE III. Conditioning and reconditioning measurements in the order they were performed with the plasma-treated hard Cu sample (pair B). The table shows the sequences of vacuum and air exposure as well as the plasma cleaning procedures in between the pulsing runs.

	Measurement	Exposure before conditioning
I	Initial conditioning	O+Ar plasma, 12 h vacuum
II	After plasma	O+Ar plasma, 24 h vacuum
III	After vacuum	21 h vacuum
IV	After air and plasma	20 h air, O+Ar plasma, 19 h vacuum
V	After air	20 h air, 19 h vacuum

Figure 7(b) shows the reconditioning curves for the plasma-treated hard Cu electrodes compared to the initial conditioning after the plasma treatment. The order of the experiments is presented in Table III. The figure shows that, after the initial conditioning, which ended with a final electric field strength near 80 MV/m, all the subsequent reconditioning runs end up in a similar saturation field regardless of the treatment prior to the reconditioning. All of the curves quickly saturate close to the final electric field strength after the BDs start regularly occurring above 60 MV/m. The saturation field is reached at around 5×10^7 pulses in each of the runs.

There are slight differences in when the BDs start occurring regularly. For measurement V of Table III (after exposure air without consequent plasma cleaning), the regular BDs begin on the lowest number of pulses, while the highest value is achieved in measurement III (reconditioning preceded by 21 h idle time in vacuum after the previous reconditioning ended).

IV. DISCUSSION

The surface contamination measurements show that the two-step plasma treatment with oxygen and argon removes impurities from the surfaces of both electrodes, albeit the effect is nullified within a few days even if the surface remains in high vacuum ($\sim 5 \times 10^{-5}$ Pa). Plasma treatment with O and without the subsequent Ar treatment was detrimental for the surface. Hence, the two-step plasma cleaning was selected: first, the O ions were used to break hydrocarbon bonds on the surfaces and then the Ar ions were used to remove the oxide layer.[28] The additional oxidation during the O plasma cleaning is also known to be highly reactive, thus prone to attract other impurities, especially when the surface is exposed to air at the standard pressure.[39]

In Fig. 3, the measurement ERDA #3 showed that the combined O+Ar treatment indeed cleaned the surfaces most effectively. Treatment with only Ar plasma was able to remove some of the impurities on the cathode, but seemingly none on the anode. However, in our study, the primary focus was on cleaning the cathode surface since it is known to be more strongly associated with triggering of BDs.[40,41]

The optical images before and after plasma cleaning [compare Figs. 4(a) and 4(b), respectively] reveal the modifications on the cathode surface caused by the plasma treatment. The brighter circular area on the cathode surface has the same size as the anode area, which has a diameter of 40 mm, while the diameter of the whole cathode surface is 60 mm. Hence, we conclude that the change in the brightness is due to exposure to the plasma since the rest of the cathode surface [dark ring around the central spot in Fig. 4(b)] was also exposed to the corresponding neutral gas and, hence, escaped the cleaning effect of the plasma. The lighter color indicates higher reflectivity and, hence indirectly, the removal of impurities (most probably cupric oxide) from the surface. The slight reddening of the same area between Figs. 4(b) and 4(c) again points out re-oxidation of the surface after the plasma treatment solely with O plasma.

The O plasma cleaning led to the appearance of yet lighter localized spots (see Fig. 5). In Fig. 8, we highlight the most prominent spots on the whole cathode surface. We found the same spots on the cathode surface after the conditioning (surface experienced BDs), see Fig. 5(b). It is noteworthy to see that there is at least one BD crater in each of the spots after the conditioning. Some of them have multiple BD craters overlapping each other. Thus, there is a positive correlation between the location of BDs and the reflective spots; however, the former are vastly more in number compared to the latter, hence the appearance of the spots cannot solely explain the triggering of the BDs.

We note that these spots are somewhat similar in size and reflectivity to the two islands seen in the top-right corner of Fig. 6(a). The islands are slightly elevated from the rest of the surface and appear after plasma treatment with O, which suggests that they are small islands of highly reflective oxidized Cu. Such thin layers of surface impurities could affect the local electric field strength, thus inducing BDs. However, the optical microscopy is not enough to confirm the composition of these spots, so further investigation is required to conclude their origin.

The initial conditioning curves shown in Fig. 7(a) follow the previously established trend,[23] where the hard Cu is conditioned much faster than the soft Cu. What is remarkable is the electric field strength at which the first BDs occur. The first BD fields at the plasma-treated surfaces are almost twice as high as those of the corresponding non-treated surfaces and more than 50% higher when comparing to all the pairs measured earlier that are comparable to these measurements. However, the conditioning slows down or even reverses after around 10^8 pulses, which amounts to 500–1000 BDs depending on the measurement.

The de-conditioning of the plasma-treated hard Cu (pair B) could be related to the poorer vacuum compared to the measurement without the treatment.[7] The Cu surfaces are also known to become activated by the plasma treatment,[38] which possibly makes them more reactive to the impurities from the vacuum and sputtering of atom clusters from the BD craters. In addition to the sputtered material from these craters, the reactive surface of the crater spot itself is exposed to the vacuum residuals. The de-conditioning trend is not seen with soft Cu. However, the overall conditioning speed of the soft Cu is lower, so the same effect could be observed simply as a more gradual slope. Further experiments with additional electrodes are needed to confirm the exact mechanism behind the de-conditioning.

The fact that the plasma cleaning has a large effect in the beginning of the initial conditioning, but a minimal effect in the reconditioning of the same electrode pair, as seen in Fig. 7(b), strengthens the hypothesis of two conditioning processes: extrinsic and intrinsic. As we saw the. plasma treatment was modifying the surface unevenly, mainly affecting the spots on the surface contaminated by impurities that are responsive to the specific plasma cleaning. It is also likely that the energetic plasma ions striking the surface might make some surface features blunter than they would be on an untreated surface. It is clear that, without cleaning, these surface features, including the contaminated spots, act as nucleation sites for the very first BDs registered when the applied voltage is still low since these are strongly reduced after the plasma cleaning. However, the fact that the saturated value of the conditioning curve returns to the same value as for the electrodes without plasma cleaning supports the hypothesis that material properties below the surface contribute to the BD generation as well. Thus, our results

indicate that even if the electrode surface is cleaned to a high degree of purity and smoothness, changes in the subsurface material such as dislocation movement still contribute to the formation of the BD spots, as supported by the models in Refs. 16–18 and 42. Such intrinsic conditioning state is achieved after the initial conditioning and does not deteriorate even after a prolonged exposure to air. We see it as the memory effect since the same saturation electric field strength is reached even during the reconditioning runs. Not only the saturation field, but also the number of pulses required to reach it, is nearly the same regardless of the electrode exposure and cleaning prior to the reconditioning, thus suggesting that the underlying intrinsic BD generation mechanism does not depend on the state of the surface.

V. CONCLUSIONS

Plasma cleaning of Cu electrode surfaces was examined with a vacuum microgap dc system. The resulting effects were studied by measuring the elemental, optical, and topographical changes on the surfaces. In addition, the surfaces were exposed to high-voltage dc pulses in order to study the breakdown generation on the plasma cleaned electrodes.

The results show that the plasma cleaning was able to decrease the amount of surface impurities. The plasma cleaning also increased the breakdown resistance of the non-conditioned electrodes by increasing the electric field strength achieved before the first BD event by more than 90% on both hard and soft Cu electrodes. However, the effect was seen to be short term and to be significant only with pristine electrodes.

Additional studies with changing voltage bias would be needed to understand the differences in the plasma cleaning effects between the anode and the cathode. Furthermore, the impact on reconditioning could be studied by filling the chamber, for example, with an inert gas instead of air, between the reconditioning runs. Moreover, high-resolution elemental analysis can help in understanding the nature of the optically observed microscopic features on the electrode surfaces due to the plasma cleaning and hence clarify their relation to the increased probability of vacuum breakdowns.

ACKNOWLEDGMENTS

The optical scanning microscope imaging related to the results was performed by Eric Brücken at the Detector Laboratory of the Helsinki Institute of Physics.

APPENDIX: NORMALIZED CONDITIONING CURVES

Comparing conditioning curves measured with different electrode gaps is not simple. It has been shown in Refs. 37 and 27 that the conditioning electric field strength does not scale with the gap size as V/d, as one would expect based on the strength of the surface electric field. Instead, the gap distance should be scaled by $\left(\frac{1}{d}\right)^{0.7}$ to precisely match the measurements.

Thus, the values shown in Fig. 7(a) were scaled according to Eq. (A1) to normalize the conditioning curves by maximum voltage and gap size. The results are shown in Fig. 9,

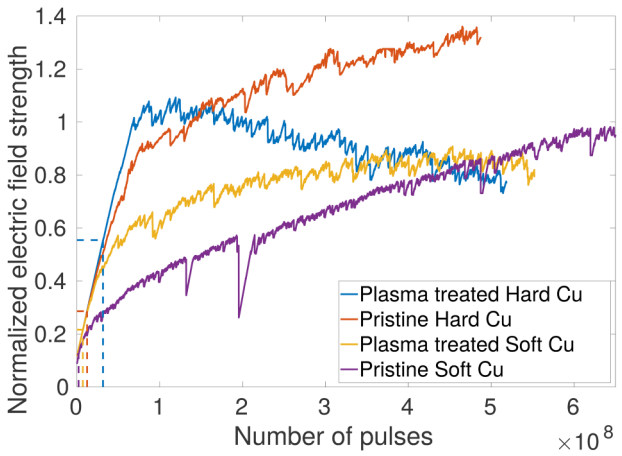

FIG. 9. Data of Fig. 7(a) normalized by the gap distances and maximum voltages according to Eq. (A1). The normalized fields and pulse numbers of the first BDs are presented in dashed lines.

$$E_{\mathrm{norm}} = \left(\frac{V}{V_{\mathrm{max}}}\right)\left(\frac{d_{\mathrm{max}}}{d}\right)^{0.7}. \tag{A1}$$

Values of $V_{\mathrm{max}} = 5249\,\mathrm{V}$ and $d_{\mathrm{max}} = 60\,\mu\mathrm{m}$ were used in the scaling.

In the case of the measurements of this work, the scaling changes the outcome very marginally. Figure 9 shows that even with the scaling, the pristine samples reach the final field much slower compared to the plasma cleaned ones. Additionally, the soft Cu samples are shown to condition slower than the hard Cu ones, as was seen also without the scaling. However, the final field strength is very similar in each of the measurements, as one would expect due to the scaling. This means that even if the values in Fig. 7(a) were based on a more simplified approach, the conclusions based on the figure are still justified.

DATA AVAILABILITY

The data that support the findings of this study are available from the corresponding author upon reasonable request.

REFERENCES

[1]D. Hoffman, B. Singh, and J. H. Thomas III, *Handbook of Vacuum Science and Technology*, edited by D. M. Hoffman, B. Singh, and J. H. I. Thomas (Academic Press, San Diego, CA, 1997), p. 20.
[2]J. A. Allen, "Oxide films on electrolytically polished copper surfaces," Trans. Faraday Soc. **48**, 273–279 (1951).
[3]M. Grunze, H. Ruppender, and O. Elshazly, "Chemical cleaning of metal surfaces in vacuum systems by exposure to reactive gases," J. Vac. Sci. Technol., A **6**, 1266 (1988).
[4]D. Peters, "Ultrasound in materials chemistry," J. Mater. Chem. **6**, 1605–1618 (1996).

[5]C. T. Walters, B. E. Campbell, and R. J. Hull, "Laser cleaning of metal surfaces," in *High-Power Laser Ablation*, edited by C. R. Phipps (International Society for Optics and Photonics, Santa Fe, NM, 1998).
[6]R. V. Latham, *High Voltage Vacuum Insulation: Basic Concepts and Technological Practice* (Elsevier, 1995).
[7]A. Saressalo, I. Profatilova, W. L. Millar, A. Kyritsakis, S. Calatroni, W. Wuensch, and F. Djurabekova, "Effect of dc voltage pulsing on high-vacuum electrical breakdowns near Cu surfaces," Phys. Rev. Accel. Beams **23**, 113101 (2020).
[8]M. Barnes, P. Adraktas, G. Bregliozzi, S. Calatroni, P. Costa Pinto, H. Day, L. Ducimetière, T. Kramer, V. Namora, V. Mertens, and M. taboretti, "High voltage performance of the beam screen of the LHC injection kicker magnets," Tech. Rep. (CERN, Dresden, Germany, 2014).
[9]I. A. Andriyash, R. Lehe, A. Lifschitz, C. Thaury, J. M. Rax, K. Krushelnick, and V. Malka, "An ultracompact X-ray source based on a laser-plasma undulator," Nat. Commun. **5**, 4736 (2014).
[10]A. Maistrello, M. Recchia, N. Marconato, T. Patton, L. Baseggio, F. Rossetto, M. Maniero, M. Pavei, E. Sartori, and G. Serianni, "Voltage hold off test of the insulating supports for the plasma grid mask of SPIDER," Fusion Eng. Des. **162**, 112055 (2021).
[11]C. Hoeber, E. Robertson, I. Katz, V. Davis, and D. Snyder, "Solar array augmented electrostatic discharge in GEO," in *17th AIAA International Communications Satellite Systems Conference and Exhibit* (American Institute of Aeronautics and Astronautics, Reston, VA, 1998).
[12]J. Bourhis, W. J. Sozzi, P. G. Jorge, O. Gaide, C. Bailat, F. Duclos, D. Patin, M. Ozsahin, F. Bochud, J.-F. Germond, R. Moeckli, and M.-C. Vozenin, "Treatment of a first patient with FLASH-radiotherapy," Radiother. Oncol. **139**, 18 (2019).
[13]A. Hull and E. Burger, "Some characteristics of the discharge between cold electrodes in vacuum," Phys. Rev. **31**, 1121 (1928).
[14]L. Snoddy, "Vacuum spark discharge," Phys. Rev. **37**, 1678 (1931).
[15]M. Aicheler, P. Burrows, M. Draper, T. Garvey, P. Lebrun, K. Peach, N. Phinney, H. Schmickler, D. Schulte, and N. Toge, "A multi TeV linear collider based on CLIC technology: CLIC conceptual design report," Tech. Rep. (CERN, 2012).
[16]K. Nordlund and F. Djurabekova, "Defect model for the dependence of breakdown rate on external electric fields," Phys. Rev. Spec. Top.–A ccel. Beams **15**, 071002 (2012).
[17]E. Z. Engelberg, J. Paszkiewicz, R. Peacock, S. Lachmann, Y. Ashkenazy, and W. Wuensch, "Dark current spikes as an indicator of mobile dislocation dynamics under intense dc electric fields," Phys. Rev. Accel. Beams **23**, 123501 (2020).
[18]M. Jacewicz, J. Eriksson, R. Ruber, S. Calatroni, I. Profatilova, and W. Wuensch, "Temperature-dependent field emission and breakdown measurements using a pulsed high-voltage cryosystem," Phys. Rev. Appl. **14**, 061002 (2020).
[19]A. Kyritsakis, E. Baibuz, V. Jansson, and F. Djurabekova, "Atomistic behavior of metal surfaces under high electric fields," Phys. Rev. B **99**, 205418 (2019).
[20]V. Jansson, E. Baibuz, A. Kyritsakis, S. Vigonski, V. Zadin, S. Parviainen, A. Aabloo, and F. Djurabekova, "Growth mechanism for nanotips in high electric fields," Nanotechnology **31**, 355301 (2020).
[21]M. Veske, A. Kyritsakis, F. Djurabekova, K. N. Sjobak, A. Aabloo, and V. Zadin, "Dynamic coupling between particle-in-cell and atomistic simulations," Phys. Rev. E **101**, 053307 (2020).
[22]R. A. Langley and J. M. McDonald, AIP Conf. Proc. **199**, 106 (1990).
[23]A. Korsbäck, F. Djurabekova, L. M. Morales, I. Profatilova, E. R. Castro, W. Wuensch, S. Calatroni, and T. Ahlgren, "Vacuum electrical breakdown conditioning study in a parallel plate electrode pulsed dc system," Phys. Rev. Accel. Beams **23**, 1–13 (2020).
[24]ASTM International, "ASTM E112-13, Standard test methods for determining average grain size" (2013).
[25]A. Saressalo, A. Kyritsakis, I. Profatilova, J. Paszkiewicz, S. Calatroni, W. Wuensch, and F. Djurabekova, "Classification of vacuum arc breakdowns in a pulsed dc system," Phys. Rev. Accel. Beams **23**, 023101 (2020).
[26]I. Profatilova, X. Stragier, S. Calatroni, A. Kandratsyeu, E. Rodriquez Castro, and W. Wuensch, "Breakdown localisation in a pulsed DC electrode system," Nucl. Instrum. Methods Phys. Res., Sect. A **953**, 163079 (2020).
[27]I. Profatilova, W. Wuensch, and S. Calatroni, "Behaviour of copper during initial conditioning in the pulsed DC system," CLIC Note (2019).
[28]R. Kohli and K. L. Mittal, *Developments in Surface Contamination and Cleaning: Applications of Cleaning Techniques*, edited by R. Kohli and K. L. Mittal (Elsevier, 2019), Vol. 11, pp. 291–305.
[29]P. Tikkanen, V. Palonen, H. Jungner, and J. Keinonen, "AMS facility at the University of Helsinki," Nucl. Instrum. Methods Phys. Res., Sect. B **223–224**, 35 (2004).
[30]U. Paaver, J. Heinämäki, I. Kassamakov, E. Hæggström, T. Ylitalo, A. Nolvi, J. Kozlova, I. Laidmäe, K. Kogermann, and P. Veski, "Nanometer depth resolution in 3D topographic analysis of drug-loaded nanofibrous mats without sample preparation," Int. J. Pharm. **462**, 29 (2014).
[31]"Manual EPULSUS-FPM1-10" (Energy Pulse Systems, 2015).
[32]V. A. Lisovsky and S. D. Yakovin, "Scaling law for a low-pressure gas breakdown in a homogeneous DC electric field," J. Exp. Theor. Phys. Lett. **72**, 34–37 (2000).
[33]M. Klas and S. Matejcík, "DC breakdown in air, oxygen and nitrogen at micrometer separations," in *HAKONE 2010—12th International Symposium on High Pressure Low Temperature Plasma Chemistry* (Department of Experimental Physics, Faculty of Mathematics, Physics and Informatics, Comenius University in Bratislava (Slovakia); Society for plasma research and applications in cooperation with Library and Publishing Centre CU, Bratislava, Slovakia, 2010), pp. 112–116; available at http://neon.dpp.fmph.uniba.sk/hakoneXII/downloads/Book_of_Contributed_Papers.pdf.
[34]M. Radmilović-Radjenović and B. Radjenović, "Theoretical study of the electron field emission phenomena in the generation of a micrometer scale discharge," Plasma Sources Sci. Technol. **17**, 024005 (2008).
[35]Y. Fu, P. Zhang, and J. P. Verboncoeur, "Paschen's curve in microgaps with an electrode surface protrusion," Appl. Phys. Lett. **113**, 054102 (2018).
[36]S. Kajita, D. Hwangbo, N. Ohno, M. M. Tsventoukh, and S. A. Barengolts, "Arc spot grouping: An entanglement of arc spot cells," J. Appl. Phys. **116**, 233302 (2014).
[37]A. Maitland, "New derivation of the vacuum breakdown equation relating breakdown voltage and electrode separation," J. Appl. Phys. **32**, 2399–2407 (1961).
[38]H. Park and S. E. Kim, "Two-step plasma treatment on copper surface for low-temperature Cu thermo-compression bonding," IEEE Trans. Compon., Packag., Manuf. Technol. **10**, 332 (2020).
[39]X. Hu, J. Schuster, S. E. Schulz, and T. Gessner, "Surface chemistry of copper metal and copper oxide atomic layer deposition from copper(II) acetylacetonate: A combined first-principles and reactive molecular dynamics study," Phys. Chem. Chem. Phys. **17**, 26892 (2015).
[40]Z. Zhou, A. Kyritsakis, Z. Wang, Y. Li, Y. Geng, and F. Djurabekova, "Direct observation of vacuum arc evolution with nanosecond resolution," Sci. Rep. **9**, 7814 (2019).
[41]Z. Zhou, A. Kyritsakis, Z. Wang, Y. Li, Y. Geng, and F. Djurabekova, "Spectroscopic study of vacuum arc plasma expansion," J. Phys. D: Appl. Phys. **53**, 125501 (2020).
[42]E. Nefedtsev and S. Onischenko, "Marks on single-crystal copper cathodes after short-pulse voltage impact on vacuum gaps," in *2020 7th International Congress on Energy Fluxes and Radiation Effects (EFRE), Tomsk, Russia* (IEEE, 2020).